### CHAPTER 133

### WAVE FORCES ON SQUARE CAISSONS

by

G.R. Mogridge\* and W.W. Jamieson\*

# ABSTRACT

The forces and overturning moments exerted by waves on large vertical square-section caissions have been measured in the laboratory. Each model caisson extended from the bottom of a wave flume through the water surface and was oriented either with one side perpendicular to the direction of wave propagation or turned through an angle of forty-five degrees to this position. For a given orientation, each model was tested for a range of wave heights (up to the point of breaking) for various wave periods and water depths. A digital computer was used for the acquisition, processing, plotting and storage of the experimental data.

In addition to the experimental work, an approximate theoretical method is presented which allows the wave loadings on a square caisson to be estimated by means of a simple desk calculation. The experimental data shows that this simple method of calculation is reasonably accurate over a wide range of wave conditions and caisson sizes.

## INTRODUCTION

In recent years, considerable research has been carried out to estimate the wave loads on various shapes of monolithic offshore structures; however, very little information is available in the literature concerning wave loadings on large vertical square-section caissons resting on the ocean bottom and extending through the water surface. Hogben and Standing (3) describe a numerical method which can be used for the solution of wave loads on large bodies including square caissons. The same method was previously used by Garrison and Chow (2), Milgram and Halkyard (7), and numerous others. Although numerical methods can be used for shapes

<sup>\*</sup> Assistant Research Officers, Hydraulics Laboratory, National Research Council of Canada, Ottawa, Ontario, Canada, KlA 0R6.

for which closed form solutions do not exist, programming is time consuming and computation costs can be high. Hogben and Standing presented a few results of wave loads measured on a model of a square caisson. The experimental data was compared with the numerical solution (4) and also an approximate solution (3) based on the diffraction theory of MacCamy and Fuchs (6). For most of the range of relative caisson sizes tested, the results fitted both solutions reasonably well. Ijima, Chou and Yumura (5) have presented a numerical method for calculation of wave scattering by isolated breakwaters of arbitrary shape. Wave height distributions about rectangular breakwaters were calculated and were found to compare favourably with distributions measured in the laboratory. Although wave forces were not measured on the model breakwaters, they were calculated using the known velocity potentials at the boundaries of the breakwaters.

In this presentation it is assumed that in general terms, the wave forces on a square caisson or cylinder occur in a similar manner to the wave forces on a circular cylinder. That is, if the size of the square cylinder is small relative to the wave length, the cylinder does not deform the incident wave and the wave force on the cylinder consists of the sum of the inertial and viscous forces. However, if the size of the cylinder or caisson is large relative to the incident wave length, it causes reflection and diffraction of the incident waves and the viscous drag forces are negligible in comparison to the inertial forces.

This paper presents an approximate theory which can be used to estimate the wave forces and moments on large vertical square caissons. The theory, based on the linear diffraction theory of MacCamy and Fuchs (6), has been simplified so that only three graphs need be used to obtain the complete solution. Force and moment measurements on models of square caissons show that the approximate theory gives a satisfactory solution over a large range of caisson sizes and wave conditions.

### THEORETICAL METHOD

It is assumed that the wave force on a large square-section cylinder or caisson can be expressed as an inertial force if the coefficient of mass used includes the effects of wave reflection and diffraction. Thus the horizontal force per unit length of the caisson is expressed as

$$f_{x} = C_{ms} pb^{2} du/dt$$
 (1)

where C  $_{\rm ms}$  is the coefficient of mass for the square-section caisson,  $\rho$  is the mass density of the fluid, b is the side length of the caisson and du/dt is the horizontal component

of the water particle acceleration. Substituting into Eq. 1 the expression for du/dt from linear wave theory gives

$$f_{x} = C_{ms} \frac{2\pi^{2}\rho b^{2}H}{T^{2}} \frac{\cosh k(y+d)}{\sinh kd} \cos (kx - \sigma t)$$
 (2)

where H is the incident wave height, T is the wave period, d is the water depth,  $\sigma$  is the wave frequency,  $\sigma=2\pi/T$ , k is the wave number,  $k=2\pi/L$ , L is the wave length and t is the time. The coordinates are chosen so that x is positive in the direction of wave propagation and y is positive in the upward direction. The origin of these coordinates is at the still water level where the water surface elevation plotted against x has a maximum negative slope (Fig. 4). By equating the inertial force per unit length on a square caisson to that on a circular caisson of diameter  $D_{\rm e}$ ,

$$C_{ms} \rho b^2 du/dt = 0.25 C_{m} \rho \pi D_e^2 du/dt$$
 (3)

it is found that the diameter of an equivalent circular cylinder is

$$D_{e'} = 2b \left( C_{ms} / \pi C_{m} \right)^{\frac{1}{2}}$$
 (4)

If it is assumed that  $C_{ms} = C_{m}$ , then,

$$D_{p} = 2b/\pi^{\frac{1}{2}}$$
 (5)

The force per unit length on the equivalent circular cylinder is obtained using the diffraction theory of MacCamy and Fuchs (6):

$$f_{x} = \frac{2\rho gH}{k} \frac{\cosh k(y + d)}{\cosh kd} A(ka_{e}) \cos (\sigma t - \alpha)$$
 (6)

where

$$A(ka_e) = \left(J_1^{'2}(ka_e) + Y_1^{'2}(ka_e)\right)^{-\frac{1}{2}}$$

$$\alpha = \tan^{-1} \left(\frac{J_1^{'}(ka_e)}{Y_1^{'}(ka_e)}\right)$$

and

g is the acceleration due to gravity,  $a_e$  is the radius of the equivalent circular cylinder, and  $J_1$  and  $Y_1$  are Bessel functions of the first and second kind respectively, both of the first order. Eq. 6 is equated to Eq. 2 for x=0 to give the expression for the coefficient of mass  $C_{ms}$  for a square caisson:

$$C_{ms} = \frac{L^2}{\pi^2 b^2} A(ka_e) \frac{\cos (\sigma t - \alpha)}{\cos \sigma t}$$
 (7)

A modified coefficient of mass  $C_{ms}^{\star}$  is defined as

$$C_{ms}^* = \frac{L^2}{\pi^2 b^2} A(ka_e)$$
 (8)

such that,

$$C_{ms} = C_{ms}^* \frac{\cos(\sigma t - \alpha)}{\cos \sigma t}$$
 (9)

The coefficient of mass  $C_{ms}$  is a function of time and varies through a wave cycle while  $C_{ms}$  is only a function of b/L (Fig. 3).  $C_{ms}$  is equal to  $C_{ms}$  when  $\alpha$  is approximately zero, that is, for b/L approaching zero or equal to 0.52. The phase angle  $\alpha$  plotted as a function of b/L is shown in Fig. 4.

The total force in the x direction is obtained by integrating the force per unit length as given by Eq. 2 for x = 0, through the depth of water from the bottom to the still water level:

$$F(t) = C_{mS} \frac{\rho \pi b^2 H L}{T^2} \cos \sigma t \qquad (10)$$

Substituting the expression for  $C_{\mathrm{ms}}$  given by Eq. 9 into Eq. 10 gives

$$F(t) = C *_{ms} *_{T^2} *_{T^2} cos (\sigma t - \alpha)$$
 (11)

The maximum force occurs when  $\sigma t = \alpha$ :

$$F_{\text{max}} = C_{\text{ms}}^* \frac{\rho \pi b^2 H L}{T^2}$$
 (12)

The overturning moment about the base of the cylinder is

$$M(t) = \int_{-d}^{0} f_{x}(y + d) dy$$
 (13)

Substituting the expression for  $f_{\rm X}$  from Eq. 2 and  $C_{ms}$  from Eq. 9 and carrying out the integration gives

$$M(t) = C_{MS}^{*} \frac{\rho g b^2 H L}{4\pi} \text{ [kd tanh kd + sech kd - 1] cos } (\sigma t - \alpha)$$
 (14)

The maximum overturning moment occurs when  $\sigma t = \alpha$ :

$$M_{\text{max}} = C_{\text{ms}}^{\star} \frac{\rho g b^2 H L}{4\pi} \text{ [kd tanh kd + sech kd - 1]}$$
 (15)

Figs. 3, 4 and 5 give the solutions to the above equations. Fig. 3 gives  $C_{m_{S}}^{\star}$  by the solution of Eq. 8 so that the maximum horizontal force may be calculated by Eq. 12. The maximum overturning moment can then be obtained directly from Fig. 5 since  $C_{m_{S}}^{\star}$  is known. The phase angle  $\alpha$  is plotted in Fig. 4 and allows the determination of F(t) and M(t) as given by Eqs. 11 and 14.

### EXPERIMENTAL METHOD

The square caisson (Fig. 1) used in the experiments was 12 in. by 12 in. in cross section and was constructed of 1/4 in. thick plexiglass. It was supported 1/8 in. above the flume bottom by a rigid 3 in. diameter steel tube clamped to a steel frame above the wave flume. A force meter was contained within the caisson and consisted of two 3/4 in, diameter stainless steel strain rods 12 in. long. The wave force on the caisson was transferred to the top strain rod through a horizontal steel bar and to the bottom strain rod through a steel base plate (Fig. 1). Foil strain gauges glued on the strain rods were aligned so that total horizontal forces could be measured in the direction of wave propagation and normal to the wave direction to give longitudinal and transverse forces, respectively. The photograph in Fig. 1 shows two brass bushings on the strain rods which make the fixed connection to the supporting 3 in. diameter steel tube. The steel plate connects the free end of the bottom strain rod to the caisson, and the steel bar which passes through apertures in the supporting tube connects the free end of the upper strain rod to the caisson. Using the two bridge outputs from the strain rods, it was possible to measure total forces and to calculate the corresponding total overturning A more detailed description of the wave force meter moments. and its calibration is given by Pratte et al. (9). From the calibration curves of the force meter, its error band was estimated to be less than ±2% over the range of forces measured. The natural frequency of vibration of the caisson in the maximum depth of water was approximately 11 Hz.

Wave profiles in the flume were measured using a non-contacting capacitive wave transducer suspended above the water surface midway between the cylinder and the flume wall. The wave flume was approximately 6 ft. wide, 4.5 ft. deep and 220 ft. long.

A limited number of tests were conducted using a square caisson 2 ft. by 2 ft. in cross section to obtain force and moment data for larger values of the relative size b/L. The model caisson was suspended from a force meter in a wave flume 12 ft. wide, 4.5 ft. deep and 162 ft. long. The force meter (Fig. 2) consisted of three aluminum strain members 3 in. in diameter. The strains in these members caused by wave loads were measured using semiconductor strain gauges forming six Wheatstone bridges. Three bridges measured strain due to bending and gave outputs proportional to longitudinal, transverse and vertical forces. Three bridges measured strain due to torque and gave outputs proportional to the moments about the three coordinate axes. A detailed description of this force meter is given by Funke (1).

Preliminary tests in the 12 ft, wave flume were carried out with a 12 in. square-section caisson (Fig. 2) to confirm experiments already conducted in the 6 ft. flume.

Wave heights were measured using a capacitive rod wave gauge at the location of the model but without the model in the flume. Thus, a different method of measuring incident wave heights was an additional check on the 6 ft. flume results.

Monochromatic waves were generated in five water depths ranging from 9.7 to 29.0 in. and nine wave periods were tested from 0.77 to 2.58 sec. For each water depth and period tested, a number of wave heights were generated ranging from small amplitude waves to those that were on the point of breaking. Each model caisson was tested with two faces parallel to the incident wave fronts ( $\beta = 0^{\circ}$ ) and also at 45° to this position ( $\beta = 45^{\circ}$ ). A digital computer was used for the acquisition, processing, plotting and storage of data. Sampling of the data was commenced after the waves passing the model reached steady state conditions. test, the wave profile and the corresponding wave forces were sampled every one hundredth of a second for a total of six seconds. Total forces and overturning moments were computed and automatically plotted along with the measured wave profile. Experimental results were also printed and data was stored on magnetic tape. Although it has not been possible to include all the experimental data in this paper, the results presented are representative of the complete testing program. A comprehensive presentation of the experimental results may be found in Mogridge and Jamieson (8).

## EXPERIMENTAL RESULTS

The number of waves in each test record varied depending on the wave period because of the fixed sampling time of six seconds. Any test with a variation in wave height or maximum force measurement within the record of more than 5% was discarded. From the test records, total forces and overturning moments were taken as average absolute maximum values of positive and negative measurements, for which the variation was normally less than 5%. The forces and corresponding moments measured in the transverse direction were negligible and are not included in the presentation of experimental results.

Using the measured absolute maximum forces with known values of wave height, length, period and caisson size,  $C_{m_{\rm S}}$  was calculated for varying values of b/L and then plotted on the theoretical curve in Fig. 3. Dimensionless moments were also calculated using the known values of  $C_{m_{\rm S}}$  and were plotted on the theoretical curve in Fig. 5. The experimental data shows good agreement with the theory for b/L between 0.092 and 0.399 and also for d/L between 0.063 and 0.786. The results shown for b/L and d/L greater than 0.09 were obtained by averaging all the test results with wave steepnesses less than 0.09. For b/L and d/L less than 0.09, only data for wave steepnesses of less than 0.01 were used. Even with this restriction on the data used, there is still some

deviation of the  $C_{MS}^{\star}$  data in Fig. 3, but the moment data in Fig. 5 shows good agreement. It is concluded that the approximate theory can be used for situations where b/L and d/L are both greater than approximately 0.09. Although there is no data presented in this paper defining the d/L limit, experiments were conducted for d/L approximately equal to 0.09 and b/L greater than 0.09 for which the experimental data agreed with the linear theory. Additional data for d/L equal to 0.08 and b/L greater than 0.09, did not fit the theoretical curve, thus defining d/L of approximately 0.09 as the limit for the theory.

To examine the variation of the forces and moments with wave steepness, they have been expressed non-dimensionally and plotted against H/L in Figs. 6 to 8. The experimental results for b/L and d/L greater than 0.09 (Figs. 6 and 7) show reasonable agreement with the theoretical curves for wave steepness up to 0.09. Fig. 8 shows data for which there is a reasonable comparison with the theoretical curves only for very low wave steepness because b/L is less than 0.09. For close agreement at high wave steepness, it is necessary for both b/L and d/L to be greater than 0.09. The largest deviation between the theory and the experimental results is approximately 85% and occurs for the moment measurement for  $\beta = 45^{\circ}$ , b/L = 0.047 and H/L = 0.032. The large differences from the linear theory for b/L and d/L less than 0.09 and large H/L are believed to be due to non-linearity of the waves and the effect of viscosity introducing drag forces of considerable magnitude. For b/L and d/L larger than 0.09, these effects are apparently negligible although at values of d/L approaching 0.09, the waves were obviously non-linear and there was flow separation at the corners of the caisson under all wave conditions.

There are two factors which are evident in the experimental results from which the data in Fig. 8 has been obtained. Firstly, the absolute values of positive and negative wave loads are no longer approximately equal. They differ from their average values by as much as 30% for the data in Fig. 8 for which b/L = 0.047 and  $\beta = 45^{\circ}$ . Secondly, the phase angles between wave load records and wave profiles do not correspond to the theoretical values for  $\alpha$  given by To illustrate this, results which compare well with the theory have been plotted in Fig. 9 and results for b/L equal to 0.047 which do not compare well with the theory have been plotted in Fig. 10. In Fig. 9, positive and negative forces are approximately equal and for all wave steepnesses the measured phase difference between the force records and the wave profiles are approximately equal to the theoretical value of  $\alpha = 8.8^{\circ}$ . Although the theoretical phase difference for the results in Fig. 10 is  $\alpha = 1.3^{\circ}$ , the measured phase difference increases to almost 50° with increasing wave steepness. This is characteristic of an increasing drag force. However, the increasing phase angle

can also be due to the non-linearity of the waves because the maximum acceleration of the fluid no longer occurs at the still water level.

Although most of the experimental results described above were obtained in a 6 ft, wide flume, some experiments were conducted in a 12 ft. flume using different equipment and techniques. Since the results are intermixed, it is necessary to show how the measurements in the two wave flumes compared. The comparison is made by repeating the same tests in each wave flume using 12 in. square caissons. The first comparison shown in Fig. 11 is for b/L = 0.184, d/L = 0.445 and  $\beta$  = 0°. The second comparison (Fig. 11) is for a series of tests where there are large deviations from the theory, that is, for b/L = 0.047, d/L = 0.115 and  $\beta$  = 0°. In both cases the data obtained in the two flumes agree closely, giving an added degree of confidence to the experimental results.

### CONCLUSIONS

An approximate method (Figs. 3, 4 and 5) based on the diffraction theory of MacCamy and Fuchs (6) has been developed to give the solution for the wave loads on a square caisson piercing the water surface. The method has been found to be satisfactory for relative caisson sizes of b/L from 0.09 to 0.40, for relative water depths of d/L from 0.09 to 0.79 and wave steepnesses up to 0.09. For b/L and d/L less than 0.09, the theoretical method cannot be used except for waves of very low steepness, because viscous drag forces and non-linearity of the waves become important. The above limits of applicability for the theory are the same whether the alignment of the square caisson is beam on to the waves,  $\beta = 0^{\circ}$ , or turned through an angle of 45° to this position.

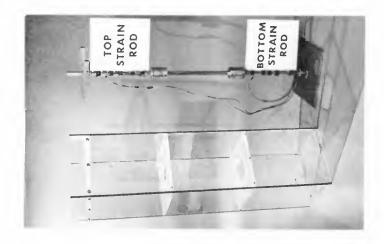
#### ACKNOWLEDGEMENT

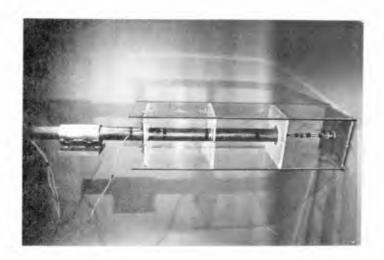
This project was funded in part by the Department of Public Works, Canada.

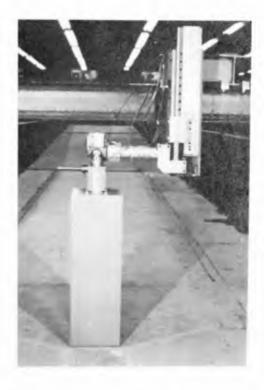
#### REFERENCES

 Funke, E.R., "A Six Degree of Freedom Dynamometer for the Measurement of Wave Forces on Models of Offshore Structures", National Research Council of Canada, Hydraulics Laboratory, Laboratory Technical Report No. LTR-HY-54, 1976.

- Garrison, C.J., and P.Y. Chow, "Wave Forces on Submerged Bodies", Proc. ASCE, Vol. 98, No. WW3, August, 1972, pp. 375-392.
- Hogben, N. and R.G. Standing, "Wave Loads on Large Bodies", International Symposium on the Dynamics of Marine Vehicles and Structures in Waves, edited by R.E.D. Bishop and W.G. Price, Mechanical Engineering Publications Limited, London, 1975, pp. 258-277.
- 4. Hogben, N. and R.G. Standing, "Experience in Computing Wave Loads on Large Bodies", Seventh Offshore Technology Conference, Houston, Paper No. OTC 2189, May, 1975, pp. 413-431.
- 5. Ijima, T., C.R. Chou and Y. Yumura, "Wave Scattering by Permeable and Impermeable Breakwater of Arbitrary Shape", Proc. Fourteenth Coastal Engineering Conference, Copenhagen, Vol. 3, Chap. 110, June, 1974, pp. 1886-1905.
- MacCamy, R.C. and R.A. Fuchs, "Wave Forces on Piles: A Diffraction Theory", U.S. Army, Beach Erosion Board, Technical Memorandum No. 69, December, 1954, 17 pp.
- 7. Milgram, J.H. and J.E. Halkyard, "Wave Forces on Large Objects in the Sea", Journal of Ship Research, Vol. 15, No. 2, June, 1971, pp. 115-124.
- Mogridge, G.R. and W.W. Jamieson, "A Design Method for the Estimation of Wave Loads on Square Caissons", National Research Council of Canada, Hydraulics Laboratory, Laboratory Technical Report No. LTR-HY-57, 1976.
- Pratte, B.D., E.R. Funke, G.R. Mogridge and W.W. Jamieson, "Wave Forces on a Model Pile", First Canadian Hydraulics Conference, Edmonton, May, 1973, pp. 523-543.







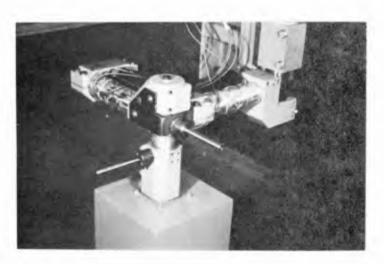


FIG.2 MODEL CAISSON AND FORCE METER (12FT WAVE FLUME)

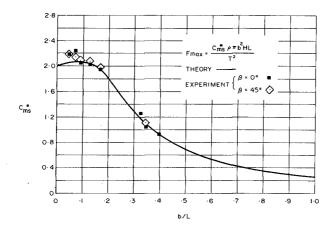


FIG. 3 Cms AS A FUNCTION OF b/L

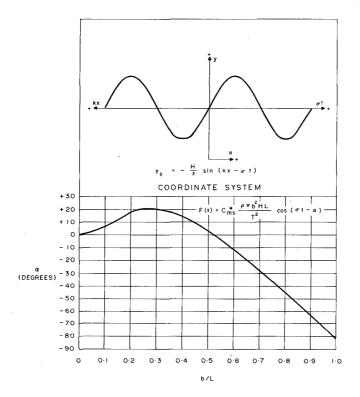
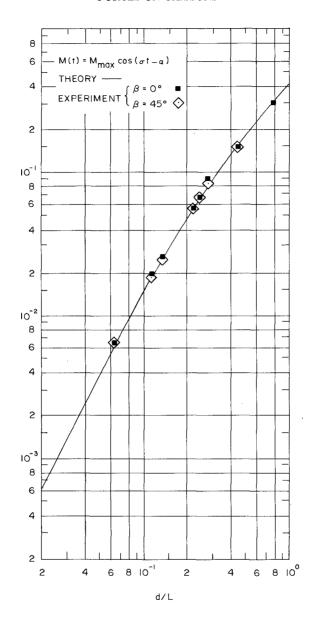
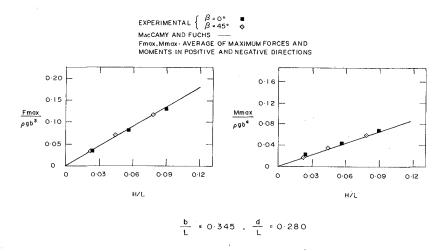


FIG. 4 PHASE ANGLE AS A FUNCTION OF b/L



 $\frac{M_{\text{max}}}{C_{\text{ms}}^* \rho g H L b^2}$ 

FIG. 5 DIMENSIONLESS OVERTURNING MOMENT AS A FUNCTION OF d/L



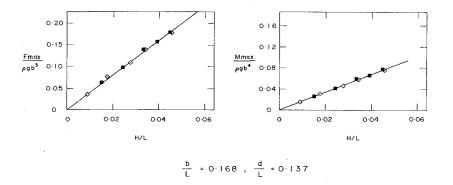


FIG.6 DIMENSIONLESS MAXIMUM FORCES AND OVERTURNING MOMENTS ON A SQUARE CAISSON

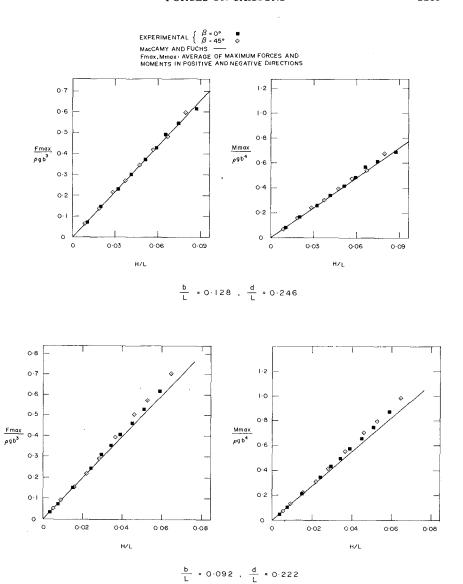


FIG.7 DIMENSIONLESS MAXIMUM FORCES AND OVERTURNING MOMENTS ON A SQUARE CAISSON

EXPERIMENTAL  $\left\{\begin{array}{l} \beta=0^{\circ} & \bullet \\ \beta=45^{\circ} & \odot \end{array}\right.$  MACCAMY AND FUCHS ——
FMOX.MOMENTS IN POSITIVE AND NEGATIVE DIRECTIONS

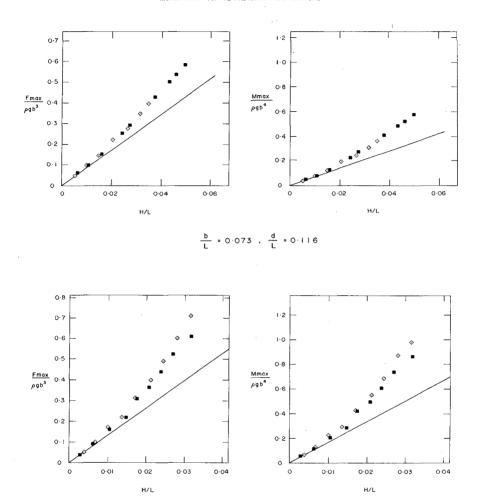
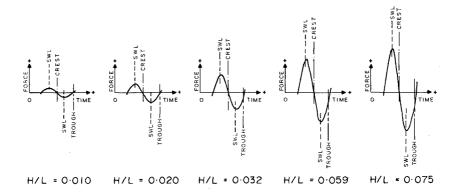


FIG.8 DIMENSIONLESS MAXIMUM FORCES AND OVERTURNING MOMENTS ON A SQUARE CAISSON

 $\frac{b}{L} = 0.047$ ,  $\frac{d}{L} = 0.115$ 



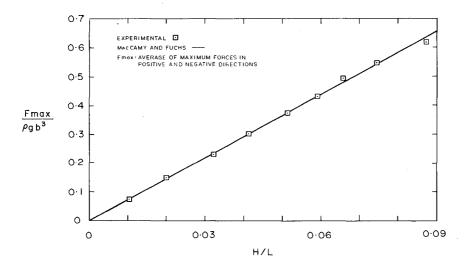
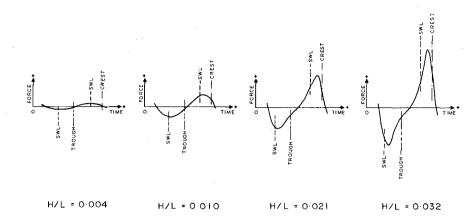


FIG. 9 PHASING BETWEEN WAVE PROFILES AND FORCE RECORDS FOR INCREASING WAVE STEEPNESS

$$(\frac{b}{L} = 0.128, \frac{d}{L} = 0.246, \beta = 0^{\circ})$$



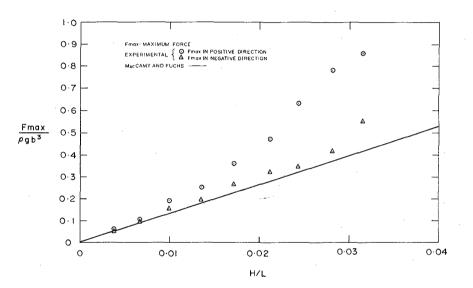
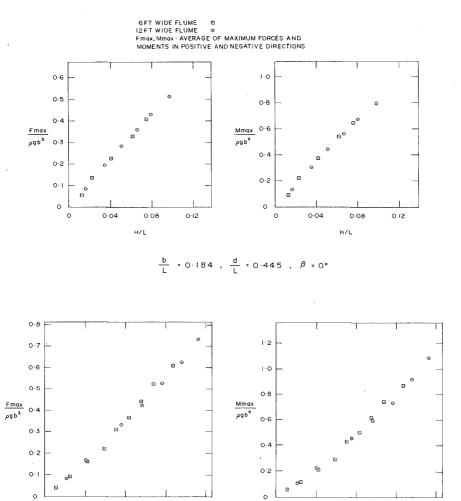


FIG.IO PHASING BETWEEN WAVE PROFILES AND FORCE RECORDS FOR INCREASING WAVE STEEPNESS

$$(\frac{b}{L} = 0.047, \frac{d}{L} = 0.115, \beta = 45^{\circ})$$



 $\frac{b}{L} = 0.047$ ,  $\frac{d}{L} = 0.115$ ,  $\beta = 0^{\circ}$ 

0.01

0.02

0.03

0.04

0.01

0.02

HZL

0.03

0.04

FIG.II COMPARISON OF TEST RESULTS USING DIFFERENT EXPERIMENTAL METHODS